PROCEEDINGS OF SCIENCE

Multiparton Interactions and Underlying Event: a PYTHIA perspective*

Christian Bierlich[a,*]

[a] *Lund University, Dept. of Astronomy and Theoretical Physics, Sölvegatan 15A, Lund, Sweden*

E-mail: christian.bierlich@thep.lu.se

We review recent developments in PYTHIA8, focused on heavy ion collisions. The ANGANTYR framework for heavy ion collisions is presented, as well as recent developments of the string shoving model for flow. It is further shown how string shoving can affect jet fragmentation in pp collisions. The effect of adding hadronic rescattering is reviewed, with focus on the nuclear modification factor, and finally ongoing work towards extending the PYTHIA8 and ANGANTYR MPI models to eletron-ion collisions is presented.

HardProbes2020
1-6 June 2020
Austin, Texas

*I thank the organizers for committing to a fully virtual conference in the face of COVID-19. Funding by the Swedish Research Council, contract number 2017-0034 is gratefully acknowledged.

*Speaker

PoS(HardProbes2020)016

1. ANGANTYR: From pp to AA

In high energy pp collisions, the PYTHIA8 [1] MPI model [2] has, since its introduction more than 20 years ago, been a staple ingredient in modeling both minimum bias collisions and underlying events. At its core, it treats pp collisions as almost independent[1] $2 \to 2$ parton collisions, with a cross section:

$$\frac{\mathrm{d}\sigma_{2\to 2}}{\mathrm{d}p_\perp^2} \propto \frac{\alpha_s^2(p_\perp^2)}{p_\perp^4} \to \frac{\alpha_s^2(p_\perp^2 + p_{\perp 0}^2)}{(p_\perp^2 + p_{\perp 0}^2)^2}, \tag{1}$$

where $p_{\perp 0}$ is a parameter regulating the low-$p_\perp$ divergence. Each sub-scattering will radiate off quarks and gluons, all connected to the beam remnants via strings [3, 4], which in turn fragment into the hadrons observed in experiments. Already in the original paper by Sjöstrand and van Zijl, it was noted that this simplistic picture of drawing two strings (for gluonic interactions) from projectile to target for all sub-scatterings, will fill the available rapidity range with too many particles. Furthermore, the isolation of MPIs must by construction ensure that quantities like the rise of $\langle p_\perp \rangle$ with multiplicity, can not be reproduced. In pp, the problems were resolved by introducing the concept of "colour reconnection", which reconnects partons from separate sub-scatterings with each other, in a way that minimizes the total string length (potential energy). We will return to colour reconnections in secs. 2 and 3, but here note that this effect is one of the main challenges faced when building up AA collisions by stacking simulated pp events on top of each other. The formalism to calculate which nucleons can interact with each other is well known due to Glauber [5] and extensions involving colour fluctuations of projectile and target [6–8], but the superimposition of partonic final states must necessarily suffer from the same problems as eq. (1) without colour reconnection. In refs. [8, 9], the ANGANTYR model was introduced, which instead of applying colour reconnection over a full pA or AA event, directly simulates sub-collisions covering only part of the available rapidity interval (with inspiration from the wounded nucleon model [10] and Fritiof [11]). Absorptively (*i.e.* inelastic non-diffractively) wounded nucleons are sorted into two classes: primary and secondary (see ref. [9] for a full description). Primary collisions are treated as normal absorptive pp collisions, and secondary collisions are treated as a single wounded nucleon, contributing as a single string with a mass distribution $\propto \mathrm{d}M^2/M^2$. This gives a good description of forward and central particle production in AA collisions. In fig. 1, ANGANTYR calculations are compared to forward production (left) as measured by ATLAS [12], as well as $\mathrm{d}N_{ch}/\mathrm{d}\eta$ for several centralities, as measured by ALICE [13, 14].

Good description of forward quantities, such as the one shown in fig. 1 (left) is key for precision comparison of Monte Carlo to heavy ion data, as it allows for an apples-to-apples comparison between theory and data, for observables binned in centrality. On the technical side, such comparisons have recently been made easier by including the necessary functionality in the RIVET framework [15, 16], as well as several other features for heavy ion analyses.

2. Shoving: A microscopic model for flow

In heavy ion collisions, multiparticle flow is taken as an indication of the formation of a deconfined plasma, with specific shear viscosity η/s smaller than any other known substance.

[1] Up to energy momentum conservation and re-scaling of parton densities of the extracted parton.

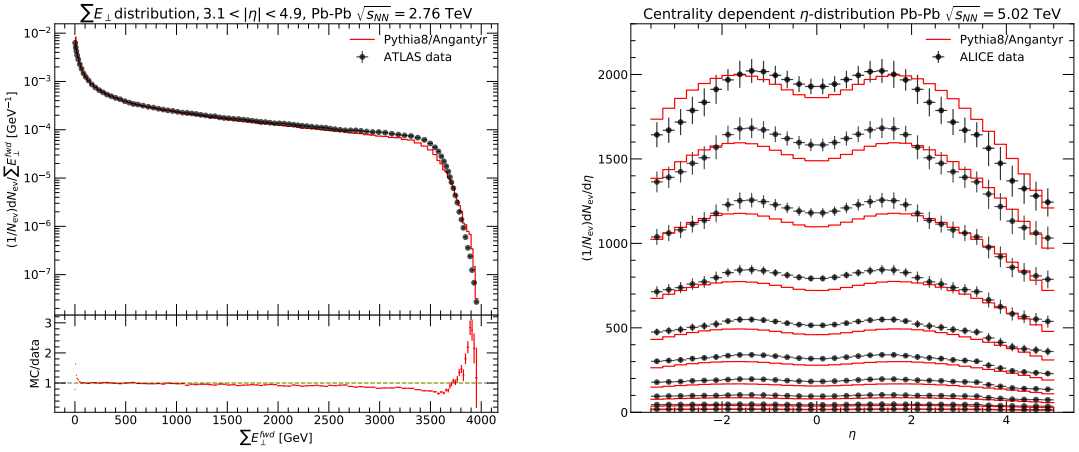

Figure 1: Forward transverse energy (left) and multiplicity as a function of pseudo-rapidity at several centralities (right) in Pb-Pb collisions at $\sqrt{s_{\mathrm{NN}}} = 2.76$ TeV shown, compared to calculation by PYTHIA8/ANGANTYR.

Discoveries at the LHC that similar features exist in high energy pp collisions, sparked investigations into whether such a plasma can also be formed in small systems [17], or whether existing models of colour reconnection can give rise to similar features [18]. While the former option is indeed a very active area, attention will here be given only to the latter. Even though also more elaborate models for colour reconnection can give rise to flow-like features [19], it can also readily be confirmed that this signature is not long-range in rapidity [20]. Moreover, there is no mechanism ensuring that measured flow coefficients encodes a response to the initial state geometry, a feature expected from heavy ion collisions. Adding to these arguments against a purely momentum-space picture of colour-reconnection, was also the realization that dense string configurations in real space, have observable consequences in high energy pp collisions, as strings will fragment as ropes [21, 22]. This became the starting point of the shoving model [23], which allows the strings' colour-electric fields to interact, resulting in strings repelling each other. The core idea that strings may interact to produce flow-like signatures pre-dates the large experimental searches [24], but the concrete model implemented in PYTHIA8 is, to our best knowledge, the only one of its kind. Other models [25] are, however, building up similar mechanisms with a momentum-space starting point.

The original Lund string concerns massless, relativistic strings which, by definition, have no transverse extension. This is well known to be an approximation – the QCD flux-tubes these strings are meant to model, have a transverse extension which can be calculated on the lattice [26]. Static properties of flux tubes on the lattice, can not directly be translated into dynamical properties of multi-string systems, and the shoving model therefore make use of the dual superconductor picture [27]. Using the duality, the classical force between two flux tubes can be calculated, provided an expression for the transverse profile of the colour electric field which, using lattice simulations, can be well approximated as:

$$E_l(x_\perp) = \frac{\Phi}{2\pi R^2} \exp\left(-\frac{x_\perp^2}{2R^2}\right), \tag{2}$$

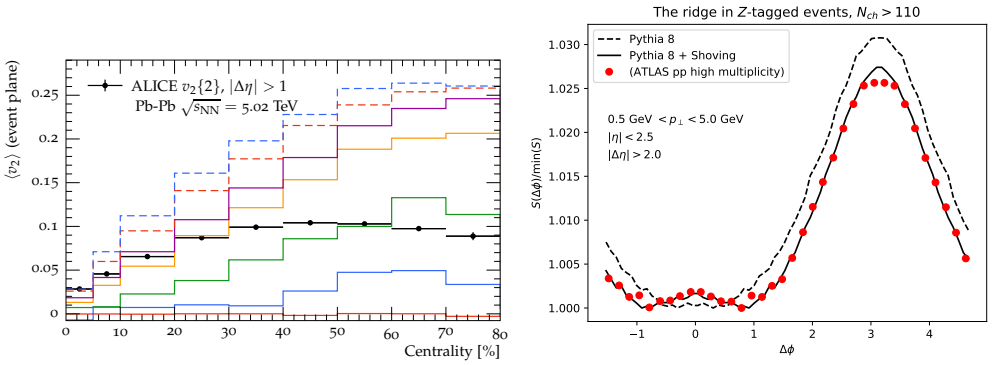

Figure 2: The v_2 flow coefficient (left) in a toy Pb-Pb event with string shoving enabled, for several string densities, compared to ALICE data. The ridge in Z-tagged pp collisions (right) compared to data from ATLAS.

where $x_\perp$ is the transverse coordinate, Φ is the flux and R is a parameter. The force per unit length of two strings with a separation $d_\perp$, can then be calculated:

$$f(d_\perp) = \frac{g\kappa}{R^2} \exp\left(-\frac{d_\perp^2}{4R^2}\right), \tag{3}$$

where g is a free parameter, determining how much of the energy goes into the magnetic current, and into breaking the condensate. The shoving model for pp collisions was presented in ref. [23], and was based on three approximations:

- All strings are straight, and parallel to the beam axis. This is a rather good approximation for low-$p_\perp$ production in high multiplicity pp collisions, but too crude for AA, and does not allow for simulation of e^+e^- collisions, where limits on flow-like signatures are being established [28, 29].
- The small nudge from one string pushing on another one, can be added by adding a soft gluon to the string.

We will concentrate here on the approximation that all strings are straight, and note that solutions to the other approximations have been presented at this conference [30].

Taking the "straight string" approximation at face value, one can construct a toy system with a purely elliptic geometry, by randomly placing straight strings, and allow them to interact. In such a geometry, flow coefficients can be calculated, as shown in fig. 2 where, on the left, v_2 is shown.

This toy simulation is compared to data from ALICE for v_2 [31], and while the comparison is not done for realistic events, it teaches the important lesson that a *local* interaction model such as string shoving, can lead to a *global* v_2.

3. Jet modifications from shoving

As indicated by the use of a toy model in Pb-Pb in the previous section, the shoving model is still best understood in pp collisions. Here, however, the model can go beyond flow coefficients, and

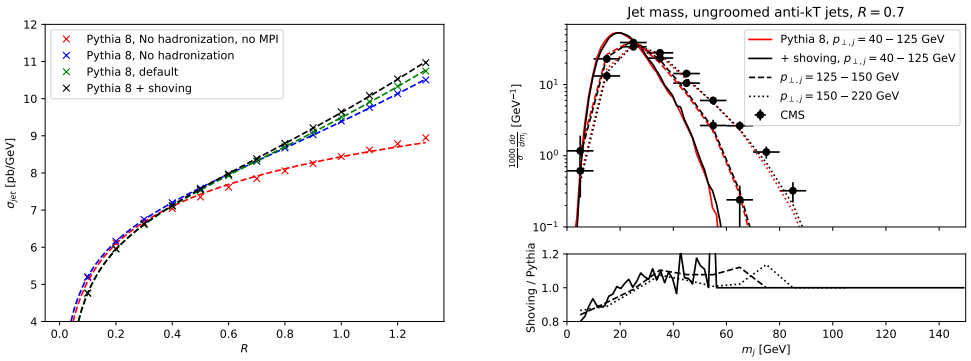

Figure 3: The jet cross section (left) in pp collisions at parton and hadron level, showing that the shoving mechanism contributes at a similar level as hadronization. The jet mass (right) compared to CMS data, pointing to the low m_j region for exploring jet modifications in small systems.

also aid in the search for jet modifications in small systems, by taking the long-range modification as a starting point, and go closer to the jet, as described in ref. [32]. Measurements by the ATLAS experiment [33] of the ridge in Z-tagged pp collisions is an interesting venue for this search, as the presence of the Z-boson ensures that some high energy scale – where also a reasonably hard balancing jet could be produced – is present in the event.

We start by confirming that the ridge in Z-tagged events can be well reproduced by the shoving model, as shown in fig. 2 (right). By construction the (leptonic) Z is not affected by shoving, as no string is stretched between the leptons. We consider now the balancing jet, defined as the leading jet found with the anti-$k_\perp$ algorithm in FastJet [34], varying the algorithms' R-parameter. In fig. 3 (left) the jet cross section, defined as:

$$\sigma_j = \int_{p_0}^{\infty} \mathrm{d}p_{\perp,j} \frac{\mathrm{d}\sigma}{\mathrm{d}p_{\perp,j}} \tag{4}$$

is shown at parton level in red (matrix element + parton shower only) and blue (with MPIs, without hadronization), and at hadron level in green (default) and in black (with shoving). Shoving has an effect on the jet cross section in pp events at a similar magnitude as hadronization, but much less than the effect from MPIs. This points out, that while a soft modification of jets due to flow-effects are expected to be present in pp collisions, the effect in traditional jet observabled will by far be overshadowed by the effect from MPIs. This makes it questionable whether standard centrality measures (proportional to particle production) will be valuable in the search for jet quenching in pp. It is furthermore seen that the effect is largest for wide (large R) jets, and searches should therefore consider focusing there.

In fig. 3 (right) a traditional calorimetric observable, the jet mass for ungroomed anti-$k_\perp$ jets with $R = 0.7$, as measured by CMS [35], is shown, and compared to PYTHIA8 with and without shoving. This result points, in addition to large R, towards the low m_j region as a suitable place for looking at small system jet modification.

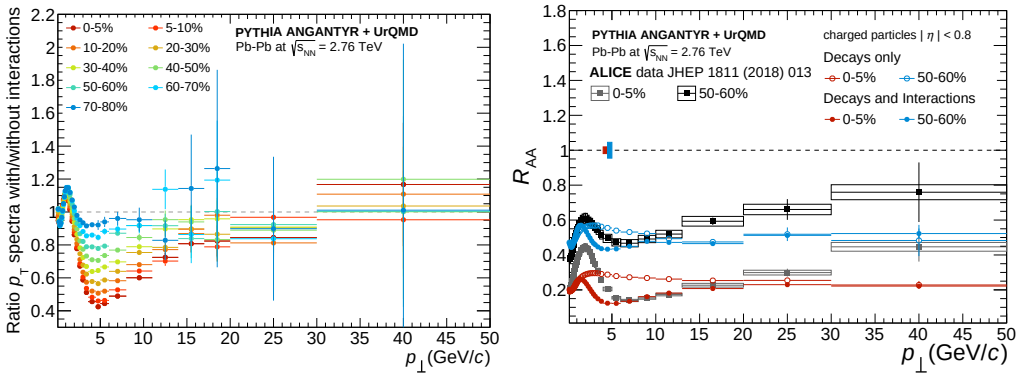

Figure 4: The effect of adding hadronic rescatterings from UrQMD in Pb-Pb collisions at $\sqrt{s_{\mathrm{NN}}}$ = 2.74 TeV. Ratio to interactions to no interactions (left) in centrality bins, and nuclear modification factor compared to data from ALICE (right).

4. Rescattering in a dense hadronic final state

Leaving aside the shoving model, similar effects on final state observables can be obtained from hadronic rescatterings. We will here present key results from ANGANTYR + UrQMD [36, 37], an attempt to make a fully plasma free "baseline", which can be used rather than simple scaled-up PYTHIA8 events in *eg.* experimental studies. In order to interface ANGANTYR with a hadronic rescattering model, having access to hadron production vertices is instrumental. We make use of the recently implemented [38] Lund string model calculation of production vertices, available in PYTHIA8.

A striking feature of the interface between ANGANTYR and UrQMD, is the very dense hadronic state undergoing rescatterings. A feature of string hadronization is a hadronization time of $\langle\tau\rangle \approx 1.4$ fm in the string rest frame, compared to $\approx$ 10 fm in hydrodynamic models. Comparatively, the hadronic re-interaction phase carries larger weight. The effect on the hadron $p_\perp$ spectrum as function of centrality, is seen in fig. 4 (left), where the ratio with/without rescattering is shown for Pb-Pb collisions at $\sqrt{s_{\mathrm{NN}}}$ = 2.76 TeV. The rescattering move particles at intermediate $p_\perp \approx$ 5-15 GeV to lower $p_\perp$, with the effect increasing for lower centralities. With a large modification on the $p_\perp$ spectrum, it is natural to construct the nuclear modification factor, shown in fig. 4 (right). Remarkably it shows very good agreement with data from ALICE [39] at intermediate $p_\perp$, which is discussed in the following.

First of all, it is clear that the ANGANTYR baseline does not follow N_{coll} scaling, as it is built on the wounded nucleon model, as presented in sec. 1. Even if the ANGANTYR model is completely wrong, the results still show a large effect on R_{AA}, which would persist irrespective of the underlying model. But a stronger conclusion is also possible. It is known that at limiting large values of $p_\perp$, N_{coll} scaling must be obeyed. But it is not known from first principles where to firmly put the separation scale between soft and hard processes. It is clear from fig. 4 (right), that ANGANTYR +UrQMD will never be able to describe the nuclear modification factor at high-$p_\perp$. Nor should it be expected to. But it does open the question whether a separation scale between soft and hard processes can be placed as high as 10-15 GeV, leaving significantly less room for partonic jet quenching effects at this scale. Several studies exist in parallel to this one, among those efforts to

implement hadronic rescattering internally in PYTHIA8 [40], as well as investigating effects on jets in the SMASH framework [41].

5. Towards MPIs in electron-ion collisions

With the planning of a future electron-ion collider becoming more concrete, it is natural to include this possibility in the ANGANTYR model. The initial work [42] involves calculating colour fluctuation corrections to the γ^*-nucleon cross section. The colour fluctuations are calculated using the Mueller dipole formalism [43], in a new Monte Carlo implementation. At the core of the calculation is the (leading order) dipole branching probability, in impact parameter space and rapidity:

$$\frac{\mathrm{d}\mathcal{P}}{\mathrm{d}y} = \mathrm{d}^2\vec{r}_3 \frac{N_c\alpha_s}{2\pi^2}\frac{r_{12}^2}{r_{13}^2 r_{23}^2}. \tag{5}$$

With a virtual photon fluctuating into a dipole as the initial state, individual Fock states can be calculated for all individual collisions. Concretely this is done as a parton shower evolution, with eq. (5) modified by a Sudakov form factor:

$$\exp\left(-\frac{N_c\alpha_s}{2\pi^2}\int_{y_{min}}^{y}\mathrm{d}y\int\mathrm{d}^2\vec{r}_3\frac{r_{12}^2}{r_{13}^2 r_{23}^2}\right).$$

The resulting cascade is ordered in rapidity, and is iterated until no further emissions are allowed without breaking a maximal rapidity, governed by the target energy and the photon virtuality. The projectile (r_{12}) and target (r_{34}) dipoles then each have an interaction probability:

$$\frac{\mathrm{d}\sigma_{dip}}{\mathrm{d}^2\vec{b}} = \frac{\alpha_s^2}{2}\log^2\left(\frac{r_{13}r_{24}}{r_{14}r_{23}}\right) \equiv f_{ij}. \tag{6}$$

Multiple scatterings exponentiate, resulting in a unitarized scattering amplitude for a single full collision:

$$T(\vec{b}) = 1 - \exp\left(-\sum_{ij} f_{ij}\right), \tag{7}$$

which leads to total cross sections, as shown in fig. 5 (left), comparing to ep cross sections from HERA.

This fixes all parameters of the model, including those governing fluctuations. With the projectile fluctuations determined for every collision, with all combinations of collision kinematics, the scattering amplitude for γ^*A collisions can be calculated. One has to appropriately take into account the transition from virtual photon to dipole, given by the photon wave function, in the first sub-collision, after which the projectile state is frozen. This is illustrated in fig. 5 (right), where the number of wounded nucleons in a γ^*Au collision is given, comparing an ordinary black disk Glauber to taking into account fluctuations and the frozen wave function. It is clearly seen that a correct calculation of fluctuations will carry importance for precise simulations for the future electron-ion collider efforts.

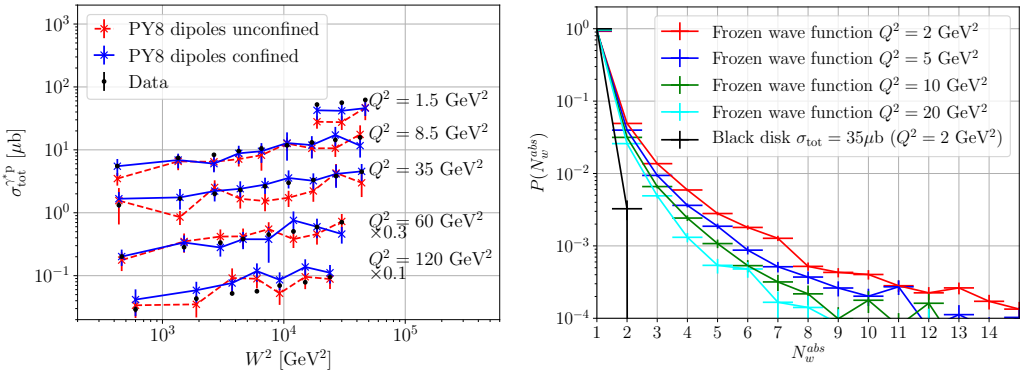

Figure 5: Estimating parameters of the dipole model (left) by fixing them to *e*p cross sections from HERE, and *e*Au Glauber model calculation (right) shoving number of wounded nucleons taking into account fluctuations in several kinematical configurations.

References

[1] T. Sjöstrand, S. Ask, J.R. Christiansen, R. Corke, N. Desai, P. Ilten, S. Mrenna, S. Prestel, C.O. Rasmussen, P.Z. Skands, Comput. Phys. Commun. **191**, 159 (2015), 1410.3012

[2] T. Sjostrand, M. van Zijl, Phys. Rev. D **36**, 2019 (1987)

[3] B. Andersson, G. Gustafson, G. Ingelman, T. Sjostrand, Phys. Rept. **97**, 31 (1983)

[4] B. Andersson, G. Gustafson, B. Soderberg, Z. Phys. C **20**, 317 (1983)

[5] R. Glauber, Phys. Rev. **100**, 242 (1955)

[6] V. Gribov, Sov. Phys. JETP **29**, 483 (1969)

[7] M. Alvioli, M. Strikman, Phys. Lett. B **722**, 347 (2013), 1301.0728

[8] C. Bierlich, G. Gustafson, L. Lönnblad, JHEP **10**, 139 (2016), 1607.04434

[9] C. Bierlich, G. Gustafson, L. Lönnblad, H. Shah, JHEP **10**, 134 (2018), 1806.10820

[10] A. Bialas, M. Bleszynski, W. Czyz, Nucl. Phys. B **111**, 461 (1976)

[11] B. Andersson, G. Gustafson, B. Nilsson-Almqvist, Nucl. Phys. B **281**, 289 (1987)

[12] G. Aad et al. (ATLAS), JHEP **09**, 050 (2015), 1504.04337

[13] E. Abbas et al. (ALICE), Phys. Lett. B **726**, 610 (2013), 1304.0347

[14] J. Adam et al. (ALICE), Phys. Lett. B **754**, 373 (2016), 1509.07299

[15] C. Bierlich et al., SciPost Phys. **8**, 026 (2020), 1912.05451

[16] C. Bierlich et al., Eur. Phys. J. C **80**, 485 (2020), 2001.10737

[17] R.D. Weller, P. Romatschke, Phys. Lett. B **774**, 351 (2017), 1701.07145

[18] A. Ortiz Velasquez, P. Christiansen, E. Cuautle Flores, I. Maldonado Cervantes, G. Paić, Phys. Rev. Lett. **111**, 042001 (2013), 1303.6326

[19] C. Bierlich, J.R. Christiansen, Phys. Rev. D **92**, 094010 (2015), 1507.02091

[20] C. Bierlich, Nucl. Phys. A **982**, 499 (2019), 1807.05271

[21] T. Biro, H.B. Nielsen, J. Knoll, Nucl. Phys. B **245**, 449 (1984)

[22] C. Bierlich, G. Gustafson, L. Lönnblad, A. Tarasov, JHEP **03**, 148 (2015), 1412.6259

[23] C. Bierlich, G. Gustafson, L. Lönnblad, Phys. Lett. B **779**, 58 (2018), 1710.09725

[24] V. Abramovsky, E. Gedalin, E. Gurvich, O. Kancheli, JETP Lett. **47**, 337 (1988)

[25] C.B. Duncan, P. Skands, SciPost Phys. **8**, 080 (2020), 1912.09639

[26] P. Cea, L. Cosmai, F. Cuteri, A. Papa, Phys. Rev. D **89**, 094505 (2014), 1404.1172

[27] M. Baker, J.S. Ball, F. Zachariasen, Phys. Rept. **209**, 73 (1991)

[28] A. Badea, A. Baty, P. Chang, G.M. Innocenti, M. Maggi, C. Mcginn, M. Peters, T.A. Sheng, J. Thaler, Y.J. Lee, Phys. Rev. Lett. **123**, 212002 (2019), 1906.00489

[29] A. Abdesselam et al. (Belle) (2020), 2008.04187

[30] S. Chakraborty (2020), 2009.00559

[31] J. Adam et al. (ALICE), Phys. Rev. Lett. **116**, 132302 (2016), 1602.01119

[32] C. Bierlich, Phys. Lett. B **795**, 194 (2019), 1901.07447

[33] M. Aaboud et al. (ATLAS), Eur. Phys. J. C **80**, 64 (2020), 1906.08290

[34] M. Cacciari, G.P. Salam, G. Soyez, Eur. Phys. J. C **72**, 1896 (2012), 1111.6097

[35] S. Chatrchyan et al. (CMS), JHEP **05**, 090 (2013), 1303.4811

[36] S. Bass et al., Prog. Part. Nucl. Phys. **41**, 255 (1998), nucl-th/9803035

[37] A.V. da Silva, W.M. Serenone, D. Dobrigkeit Chinellato, J. Takahashi, C. Bierlich (2020), 2002.10236

[38] S. Ferreres-Solé, T. Sjöstrand, Eur. Phys. J. C **78**, 983 (2018), 1808.04619

[39] S. Acharya et al. (ALICE), JHEP **11**, 013 (2018), 1802.09145

[40] T. Sjöstrand, M. Utheim (2020), 2005.05658

[41] P. Dorau, J.B. Rose, D. Pablos, H. Elfner, Phys. Rev. C **101**, 035208 (2020), 1910.07027

[42] C. Bierlich, C.O. Rasmussen, JHEP **10**, 026 (2019), 1907.12871

[43] A.H. Mueller, Nucl. Phys. B **415**, 373 (1994)